


Improving the precision and accuracy of wildlife monitoring with multi-constellation, multi-frequency GNSS collars

María S. Garrido-Carretero¹  | Concepción Azorit² |
María C. de Lacy-Pérez de los Cobos³ |
José Manuel Valderrama-Zafra⁴ | Rafael Carrasco² |
Antonio J. Gil-Cruz¹

¹Department of cartographic, geodetic and photogrammetric engineering, University of Jaén, Las Lagunillas Campus, Jaén 23071, Spain

²Department of animal, vegetal biology and ecology, University of Jaén, Las Lagunillas Campus, Jaén 23071, Spain

³Department of statistics and data science, San Pablo CEU University, Madrid 28003, Spain

⁴Department of engineering graphics, design and projects, University of Jaén, Las Lagunillas Campus, Jaén 23071, Spain

Correspondence

María S. Garrido-Carretero, Department of cartographic, geodetic and photogrammetric engineering, University of Jaén, Las Lagunillas Campus, Jaén 23071, Spain.
Email: mgarrido@ujaen.es

Funding information

MINECO of Spain, Grant/Award Number: Project CGL2016-78577-P; Junta de Andalucía, Grant/Award Numbers: PAIDI2020, P20-00897, P07-RNM-03087, RNM282-RNM175; Universidad de Jaén, Grant/Award Numbers: Funding for open access charge UJA/CBUA, POAIUJA 2021-2022 and CECTEMA, Programa Operativo FEDER Andalucía 2014-2020

Abstract

The use of global navigation satellite systems (GNSS) technology within the fields of ecology and biology has increased over recent years. With Global Positioning System, GLObalnaya NAVigatsionnaya Sputnikovaya Sistema, Galileo, and BeiDou systems fully deployed, >140 navigation satellites are currently available for navigation and high precision positioning applications. The technological improvements in GNSS devices, mainly due to the multi-frequency capability, reduce signal acquisition time and increase the reliability, the continuity, and the accuracy of the estimated position, especially in complex environments like forests or areas with a steep topography. This study aims to test experimentally the influence of multi-constellation multi-frequency modules on the performance of the GNSS collars used to monitor wildlife. We applied static and kinematic tests designed to assess and compare the performance of GNSS collars equipped with a single-frequency versus a multi-frequency chipset. We evaluated the availability and continuity of solutions, number of satellites used, dilution of precision, precision, accuracy, and repeatability of these quality parameters for GNSS devices in southeastern Spain

This is an open access article under the terms of the Creative Commons Attribution-NonCommercial-NoDerivs License, which permits use and distribution in any medium, provided the original work is properly cited, the use is non-commercial and no modifications or adaptations are made.

© 2023 The Authors. *The Journal of Wildlife Management* published by Wiley Periodicals LLC on behalf of The Wildlife Society.

from February 2021 to June 2022. The results confirmed that the multi-constellation multi-frequency GNSS collar showed a stable and good performance in terms of the number of satellites used (>10), horizontal dilution of precision (<1.3), fix success rate (100%), mean location error (<1.5 m), and circular error probability (CEP), which was better by approximately one order of magnitude than the single-frequency collar (1–10 m). The use of reliable and accurate GNSS devices will expand our knowledge of animal behavior and the interactions between species. Multi-frequency GNSS collars allow collection of accurate locations, providing fine-scale information about animal behavior (e.g., feeding strategies, competition for resources), whereas the single-frequency GNSS collars can be used for broad-scale studies (e.g., home ranges, habitat use).

KEYWORDS

global navigation satellite systems, GNSS collar, kinematic positioning, location device, multi-frequency, single-frequency, static positioning, wildlife monitoring

The term global navigation satellite system (GNSS) covers each individual satellite-based positioning system and the combination of several systems (Hofmann-Wellenhof et al. 2008). A GNSS system is composed of a constellation of satellites and a control station network. These satellites broadcast to GNSS devices the time and orbital information for navigation and positioning applications (Alonso et al. 2020, Caporali and Zurutuza 2021). Currently there are 4 global positioning satellite systems deployed: the United States Global Positioning System (GPS), the Russian GLObalnaya NAVigatsionnaya Sputnikovaya Sistema (GLONASS), the European Galileo system, and the Chinese BeiDou system. These systems lead to a multi-constellation and multi-frequency system denoted as multi-GNSS (Teunissen and Montenbruck 2017). A detailed description of the space segment can be found in Pan et al. (2019). Once the GPS, GLONASS, Galileo, and BeiDou systems are fully deployed, >140 satellites will be available for navigation and positioning applications (Li et al. 2022). The number of GNSS signals and services already deployed has enabled new levels of performance in terms of accuracy, covering a wide range of application areas such as surveying and geomatics (Garrido et al. 2018, 2019; Tunini et al. 2022), engineering (Barzaghi et al. 2018, Pipitone et al. 2018, Xiao et al. 2019), and environmental science (Awange 2018), and recent studies show the advantages of multi-constellation solutions considering several GNSS positioning techniques (Gao et al. 2019, Liu et al. 2020, Dardanelli et al. 2021, Li et al. 2021, Paziewski et al. 2021). With the current multi-constellation scenario, a GNSS device previously able to receive satellite signals from about 8 GPS satellites under open sky can now access more than 30 satellites, albeit at the cost of reduced battery life. More satellites and more available signals improve the accuracy of the position. In addition, the availability of a greater number of satellites allows the GNSS receiver to choose the best geometrically distributed subset to obtain a highly accurate solution (Weiss 2021). Furthermore, multi-frequency data integration leads to higher accuracy, shorter convergence time, and improved ambiguity resolution performance (Geng and Guo 2020, Xin et al. 2020, Psychas et al. 2021).

A single GNSS receiver measures the pseudorange to visible satellites and determines the receiver's position (longitude, latitude, and height) to within a few meters, and the clock bias in single point positioning mode. The error sources affecting GNSS signals and therefore the position estimation are assigned to 3 main groups (Seeber 2003):

satellite errors (satellite clock and satellite orbit), receiver error (receiver clock noise), and signal propagation errors (ionosphere, troposphere, and multipath; Figure 1). The ionosphere is a dispersive media; thus, the GNSS signal's refraction depends on its frequencies. This effect can be minimized by combining different frequencies (ionosphere-free combination model). For a single-frequency receiver, the ionospheric delay is the dominant pseudorange error. The troposphere also produces a delay in GNSS signals. Because the troposphere is a non-dispersive media, this effect depends on the GNSS signal path. It can be modeled as a function of the satellite elevation angle. Several tropospheric models (e.g., Sastamoinen, Hopfield) are available in the scientific literature (Xu 2007). Multipath occurs when GNSS signals are reflected off a surface or by objects near the GNSS antenna, such as trees. The reflected signals interfere with the signals that arrive directly from the satellites, which is one of the main sources of error in the forest environment (Grala and Brach 2009). Multipath affects both carrier-phase and pseudorange measurements and can be reduced by mitigating the GNSS signals from low elevation.

The technological improvements in GNSS devices, mainly due to their multi-frequency capability, reduce the signal acquisition time and increase the availability, reliability, continuity, and accuracy of the GNSS positioning, especially in complex environments such as mountainous areas and the forest environment (Pan et al. 2019). Multi-frequency code and phase GNSS modules offer new opportunities to current applications and open the door to emerging applications that require high accuracy. One application of GNSS technology that can benefit from multi-GNSS modules is monitoring wild animals with satellite collars. Wild animal location technologies have evolved considerably in the last decades. Since the 1990's, the use of GPS collars to study and monitor wildlife has steadily grown, and the literature demonstrates the varied information that can be gained from GPS collar-based research (Rodgers et al. 1996, Bowman et al. 2000, Rodgers 2001). Satellite-based technologies used to date, however, have their limitations and inconsistent collar performance (data loss from failed fixes and location inaccuracy or error) can produce data that are not suited for all ecological questions, or can lead to biased results if analyzed without accounting for data quality. In addition, habitat characteristics and animal behavior influence signal transmission, affecting the fix success rate and the location error (Cain et al. 2005). Frair et al. (2010) show that some parameters such as home-range estimates are robust to location imprecision. Nevertheless, habitat-biased locations and imprecise movement paths, also affected by the fix interval, may become unsuitable for ecological analyses. The recent scientific literature contains numerous examples of how GPS collar data are used in wildlife monitoring for

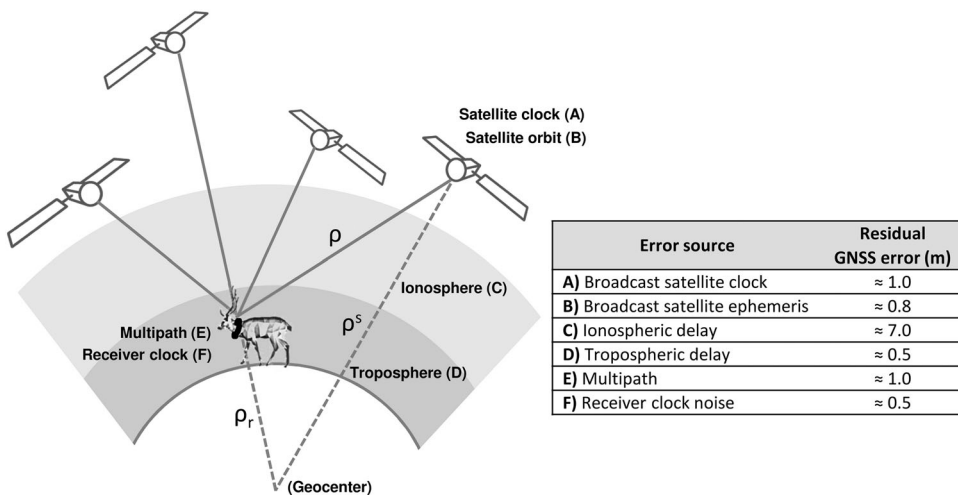


FIGURE 1 Error sources affecting global navigation satellite system (GNSS) signals and typical magnitudes of residual GNSS error. ρ^s is the space vector relative to the geocenter, ρ_r is the geocentric position vector of the GNSS device, and ρ is the geometric range to each satellite.

habitat modeling (Laguna et al. 2021), and identifying animal movement and landscape use (Wittemyer et al. 2019, Gray et al. 2022), migratory strategies (Peterson et al. 2022), predation sites (Irvine et al. 2022), birth sites (Dion et al. 2019, Marchand et al. 2021, Hooven et al. 2022), and capture locations (Hampton et al. 2020, Bengsen et al. 2021), or to define social behavior (Davis et al. 2018, Wielgus et al. 2021). Improvements to GNSS technology allow for more reliable data collection from collars; thus, new ecological questions can be investigated. Currently, GNSS devices have the potential to collect large amounts of animal tracking solutions, 24 hours per day, under all weather conditions and even unfavorable conditions due to topography, vegetation cover, or animal behavior.

This study focuses on positioning improvements introduced by a multi-constellation multi-frequency module into a GNSS collar. The main objective was to evaluate the collar performance, comparing the location errors and other quality parameters from GNSS collars equipped with single-frequency or multi-frequency GNSS modules using static and kinematic tests. The hypothesis of this study was that the multi-constellation multi-frequency GNSS collar provides precise and fine-scale information compared with the single-frequency collar.

STUDY AREA

This study was carried out in the province of Jaén (southeastern Spain) from February 2021 to June 2022. The study area is characterized by a topography that combines hills and valleys with a Mediterranean forest cover, moderately disturbed by conventional olive groves and pine plantations, and shows a multifunctional landscape characterized by a variety of forestry, agrarian, and livestock uses. It has a continental Mediterranean climate with mild winters and long, hot and dry summers, often resulting in periods of drought. The few rainfall events are concentrated in spring and autumn. The study area is home to a varied group of herbivores such as the rabbit (*Oryctolagus cuniculus*) and ungulates such as the wild boar (*Sus scrofa*) and the domestic and wild goat (*Capra pyrenaica*) and red deer (*Cervus elaphus*), carnivores such as the fox (*Vulpes vulpes*) and protected species, including the Bonelli's eagle (*Aquila fasciata*) and the goshawk (*Accipiter gentilis*).

The static tests were carried out at the Campus of the University of Jaén (37°47'16"N, 3°46'40"W), at an elevation of approximately 455 m above mean sea level (Figure 2A). For the kinematic tests, we selected 3 routes, R1, R2, and R3, along 3 mountainous areas in a rural environment of the province of Jaén (Figure 2B). The first area (37°46'48"N, 3°50'3"W), bounded by R1, covers 120 ha with an elevation ranging from 579–735 m above mean sea level. The second one, R2 (37°36'6"N, 3°45'24"W), is 2,320 ha and has an elevation above mean sea level from 927–1,516 m. The last one, R3 (37°42'32"N, 3°41'31"W), covers 12,400 ha with a mean elevation of 850 m above mean sea level.

METHODS

GNSS devices

We used 4 different GNSS devices in this study: 2 ground-based receivers and 2 collars (Figure 2). The geodetic GNSS equipment was composed of a Leica Geosystems GR10 receiver and a LEIAR10 geodetic-grade antenna with a large ground plane and built-in radome (Leica Geosystems, St. Gallen, Switzerland). The general application of this GNSS antenna is in continuously operating reference stations (CORS) and for high accuracy positioning applications. The GR10 receiver is able to observe up to 60 satellites and support parallel tracking of multiple signals, including GPS (L1/L2P/L2C/L5), GLONASS (L1/L2/L3/L5), Galileo (E1/E5a/E5b/E6), and BeiDou (B1/B2/B3). Under standard conditions, the nominal accuracy (root mean square) in differential phase static mode, baseline up to 30 km, is 5 mm + 0.5 ppm for horizontal components and 10 mm + 0.5 ppm for vertical components (Leica Geosystems 2011). We used this GNSS device in the static test to estimate the reference positions.



FIGURE 2 A) Location of geodetic pillars STB2 and STB3 for the static test carried out at the Campus of the University of Jaén, Spain, from 16–25 February 2021 showing the geodetic global navigation satellite system (GNSS) receiver and antenna (A1), the low-cost GNSS receiver and active patch antenna (LCR; A2), the multi-frequency GNSS collar (MFC; A3) and the single-frequency GNSS collar (SFC; A4). B) Routes R1, R2, and R3 for the kinematic test carried out in Jaén, Spain, in June 2021 and 2022 showing the equipment for route R1 (LCR, MFC and SFC, laptop and backpack; B1) and equipment and vehicle for routes R2 and R3 (B2).

The low-cost multi-frequency GNSS receiver (LCR) is an U-blox C099-F9P application board that includes a ZED-F9P high precision positioning module (U-blox, Thalwil, Switzerland). This receiver, offering wide usability, has become the subject of extensive research (Hamza et al. 2021, Janos and Kuras 2021, Wielgocka et al. 2021). With an active multi-band GNSS patch antenna with a magnetic base, the ZED-F9P GNSS module tracks all GNSS constellations and processes GPS (L1C/A, L2C), GLONASS (L1OF, L2OF), Galileo (E1B/C, E5b), and BeiDou (B1, B2) signals. To mitigate the multipath effect, the patch antenna must be installed on a 10-cm-diameter metallic ground plane. Anti-jamming and anti-spoofing algorithms are also implemented to discard unwanted signals (U-blox AG 2021a). The U-center free software (U-blox AG 2021b) allows us to configure and manage the receiver and to collect the output messages and coordinates. The manufacturer specifies as a term associated with the horizontal position accuracy a circular error probability (CEP) equal to 1.5 m for 24 hours of static observation (U-blox AG 2020). The CEP probability is 50%. The circular standard deviation, σ_c (39.4% probability), is a function of the standard deviations for a horizontal station (Equation 1).

$$\sigma_c \simeq (1/2)(\sigma_N + \sigma_E) \quad (1)$$

The conversion factor between σ_c and CEP for the normal circular distribution is 1.1774 (Greenwalt and Shultz 1962; Equation 2).

$$\text{CEP} = 1.1774 \sigma_c \quad (2)$$

We tested 2 GNSS collars in this study, with a similar design and components but with different GNSS modules and performance. Both collars included a GNSS module and an antenna, a microprocessor, and ancillary electronic components joined to additional sensors. Each collar had a unique serial number, which is inserted into all the data file names produced. The collar position information is extracted from the National Marine Electronics Association (NMEA) sentences. The main difference between the collars was that the multi-frequency GNSS collar (MFC) was equipped with the same ZED-F9P module and active multi-band patch antenna as the LCR; thus, we expected similar horizontal position accuracy. The single-frequency GNSS collar (SFC) was equipped with a U-blox IT530M module and a patch antenna. This multi-GNSS module receives GPS (L1C/A), GLONASS (L1), and QZSS (L1C/A) signals. Although it is a single-frequency module, by using GPS and GLONASS satellites in parallel it can enhance the position availability in obstructed satellite visibility conditions. The position accuracy (CEP) stated by the manufacturer is 3.0 m (U-blox AG 2013). The accuracies reported by manufacturers correspond to ideal conditions. Real atmospheric conditions, the multipath effect, satellite visibility, and constellation geometry lead to higher values. We used the LCR to evaluate the MFC performance in the static test and to define the reference tracks in the kinematic test.

Static and kinematic tests

To assess the performance of the GNSS devices in static mode, we conducted the test at 2 geodetic pillars located on the Science and Technology building at the Campus of the University of Jaén, identified as STB2 and STB3. They have a high precision monumentation, good sky visibility, and a free multipath environment. Each geodetic pillar is composed of a cylinder, 1.20 m high and 0.30 m in diameter, supported on a concrete base with a reinforced center to ensure accurate and stable placement of GNSS devices.

In the kinematic tests, we moved the GNSS collars through a forest and mountain environment to simulate the trajectory of a wild mammal. We traversed 3 routes, identified as R1, R2, and R3, on foot (R1) and by car (R2 and R3) to analyze the performance of the GNSS devices in motion. We walked the 6.3-km R1 route along a footpath with a normal walking speed to simulate animal movement. We drove the 25.8-km R2 route along a forest track with an average speed of 20 km/hour. We drove the 50-km R3 route along forest tracks and country roads with an average speed of 30 km/hour. We collected the 3 tracks with the LCR, MFC, and SFC simultaneously, so we assumed no differences in their observation conditions.

The performance of a GNSS device is characterized by several statistical quality parameters. Usually, the certification procedures assume a position log file over a long time interval at a known position or over a known trajectory in kinematic tests. The GNSS data, including the Coordinated Universal Time (UTC) acquisition time, the position, and the number of satellites tracking are logged under different scenarios. To analyze the GNSS positioning performance with a low-cost GNSS receiver and 2 GNSS collars, we selected the availability and the continuity of the solutions, the number of satellites used, the dilution of precision (DOP), the precision, the accuracy, and the repeatability of quality parameters. The availability of the solution or GNSS successful fixes is the ability of a GNSS device to provide a position within the coverage area. This term is related to the GNSS collars (SFC and MFC). The collar position is always estimated using single point positioning with code pseudorange observations. The continuity is the ability to perform its function without interruptions during the estimated useful life of the battery. This parameter is evaluated by the fix success rate, dividing the number of successful fixes by the number of fix attempts (Fischer et al. 2018). The number of satellites used is the number of satellites considered for

the receiver position calculation. In GNSS positioning, a good satellite geometry is crucial to guaranteeing the solution's robustness. The DOP is a description of the purely geometrical contribution to the position uncertainty. It indicates the geometrical strength of the satellite constellation at the time epoch of the measurement (Gao et al. 2017). This dimensionless parameter decreases when conditions are favorable. Standard terms are the horizontal dilution of precision (HDOP) and the vertical dilution of precision (VDOP). A low number of satellites produces high HDOP and VDOP values that decrease the positioning accuracy. Values under 2 are considered optimal values. Precision and accuracy represent qualitative concepts. The accuracy provides the conformance between an estimated GNSS position and the true position (the reference position determined with a highest level of accuracy). According to the International Organization for Standardization (2012), the measurement error is the difference between the measured value (GNSS position collected) and the reference value (estimated reference position). Thus, one position is more accurate than another if the measurement error is smaller. The mean value of the measurement error for the north and east components is computed. The horizontal accuracy is evaluated by the mean location error, which is the mean Euclidean distance between each GNSS collar position and the reference position (Forin-Wiart et al. 2015). The precision describes the dispersion of the calculated collar positions for a GNSS collar that remains stationary. Precision is calculated in terms of the circular standard deviation (σ_c) and the circular error probability (CEP), based on the standard deviation for the north and east components (σ_N and σ_E). To analyze the repeatability of the quality parameters, we conducted 3 independent observation sessions corresponding to 3 consecutive days. At each test site, we performed the GNSS survey under repeatability conditions: the same observer and the same GNSS devices used under the same conditions, the same location, and over a short period of time (Taylor and Kuyatt 1994). We used 2 independent position samples from 2 observation sessions using the same GNSS collar to determine if the differences between the mean location errors were significant (0.05 significance level) using a student's *t*-test (Teunissen 2000).

For the static tests, we placed the GNSS devices on the geodetic pillars under open-sky conditions (Table 1). To estimate the reference positions, we placed 2 geodetic GNSS receivers at the geodetic pillars STB2 and STB3. The preliminary session (S0) was a 24-hour session with a 30-second sampling rate. To compare the performance of the LCR and the MFC (test A), we used 3 independent observation sessions, 8 hours per session, at pillars STB2 and STB3, identified as S1, S2, and S3. For each session, we established a 10-minute fix rate, completing a sample size of

TABLE 1 Description of the static and kinematic tests and the observation sessions (S0 to S9) carried out in Jaén, Spain from February 2021 to June 2022 with a geodetic global navigation satellite systems (GNSS) receiver, a low-cost multi-frequency GNSS receiver (LCR), a multi-frequency GNSS collar (MFC), and a single-frequency GNSS collar (SFC).

Test	Test ID	Session ID	Date (DOY-Day of the year)	Length	GNSS device (Geodetic site or route)
Static	-	S0	15 Feb 2021 (046)	24 hr	Geodetic (STB2 and STB3)
	A	S1	16 Feb 2021 (047)	8 hr	LCR (STB3) and MFC (STB2)
		S2	17 Feb 2021 (048)	8 hr	LCR (STB3) and MFC (STB2)
		S3	18 Feb 2021 (049)	8 hr	LCR (STB3) and MFC (STB2)
	B	S4	18 Feb 2021 (049)	24 hr	MFC (STB2)
		S5	25 Feb 2021 (056)	24 hr	SFC (STB3)
Kinematic	C	S6	18 Jun 2021 (169)	90 min	LCR, MFC and SFC (R1)
		S7	19 Jun 2021 (170)	90 min	LCR, MFC and SFC (R2)
		S8	20 Jun 2022 (171)	100 min	LCR, MFC and SFC (R2)
		S9	20 Jun 2022 (171)	100 min	LCR, MFC and SFC (R3)

48 positions per session. At each fix attempt, the GNSS collar is programmed to collect satellite information for a maximum of 240 seconds. We collected positions from the LCR using a 1-second sampling rate and extracted positions from U-center software identifying the common UTC epoch with the MFC. In addition, we performed 2 sessions of 24 hours, not simultaneous (S5 and S6), with GNSS collars to highlight the improvements introduced by the multi-frequency GNSS module compared to a single-frequency module (test B). We maintained the 10-minute fix rate, expanding the sample size to 144 records. Both GNSS collars are programmed to retain satellite information before attempting a fix location in continuous mode, following standard GPS collar settings (Moriarty et al. 2015). For the accurate determination of the reference coordinates, we processed the 24-hour receiver independent exchange format (RINEX) files in precise point positioning mode (Zumberge et al. 1997) using the open-source RTKLib software version 2.4.3 (Takasu 2010). In precise point positioning mode, RTKLib applies an extended Kalman filter estimation process (Gelb 1974). The precise point positioning solution is based on the ionosphere-free combination with undifferenced observations from GNSS satellites. The method uses precise ephemeris, phase center offset, and phase center variation provided by the International GNSS Service and applies a tropospheric model to remove the tropospheric effect with estimated zenith total delay. The initial phase ambiguity is estimated as a float value. To avoid multipath effects, a cut-off angle of 8° is used. Once the GNSS data are processed and a reference value (true position) is estimated for each test site, the geocentric (X, Y, Z) or geodetic coordinates (latitude, longitude, and ellipsoid height) of all positions collected by GNSS devices are transformed into their horizontal components north and east. Although surveys performed with GNSS devices yield 3-dimensional coordinates in the geocentric system, for convenience these coordinates are converted to geodetic coordinates (Meyer 2010). Considering a reference position with geocentric coordinates $(X, Y, Z)_R$, and a GNSS position registered with coordinates $(X, Y, Z)_i$, it is common practice to transform the 3-dimensional components $(\Delta X, \Delta Y, \Delta Z)$ into a local geodetic system of north, east, and vertical components. The local geodetic system is centered on the reference position and the north and east axes are on a local horizontal plane. The local or topocentric system is linked to the geocentric coordinate system through a set of 3-dimensional rotations (Ghilani and Wolf 2010). Considering the reference position estimated by the precise point positioning mode, N_i and E_i represent the measurement error in the north and east components respectively of the i th position registered. One sample of components (N, E) is generated per session (Figure 3).

To analyze the GNSS collars performance in motion, we compared the successful fixes from the MFC and the SFC collected at the closest UTC time epoch with a reference track. We defined the reference tracks for R1, R2, and R3 using the LCR at a scheduled fix rate of 1 second. Both GNSS collars are programmed with a 10-minute fix rate to obtain evenly spaced locations. Moreover, Moriarty and Epps (2015) suggest that short fix intervals can reduce GPS error by retaining satellite information and can increase the amount of data collected on free-ranging mammals associated with areas of vegetation cover. We report the same evaluation parameters as for the static tests: the number of successful fixes, the fix success rate, the number of satellites used, and the HDOP. We computed relative accuracy as the relative location error, the shortest distance from corresponding positions from GNSS collars to the reference GNSS track (polyline generated by the segments defined by each pair of consecutive positions obtained with the LCR). We conducted 4 kinematic observation sessions, S6 to S9, over routes R1, R2, and R3 (Table 1). To analyze the repeatability of the kinematic results, we conducted 2 independent observation sessions on route R2 (S7 and S8).

RESULTS

Static tests

In test A comparing LCR and MFC, both GNSS devices showed a 100% fix success rate. The mean location error was 0.464–0.751 m for the LCR and 1.36–1.40 m for MFC (Table 2) resulting in more clustered estimated positions

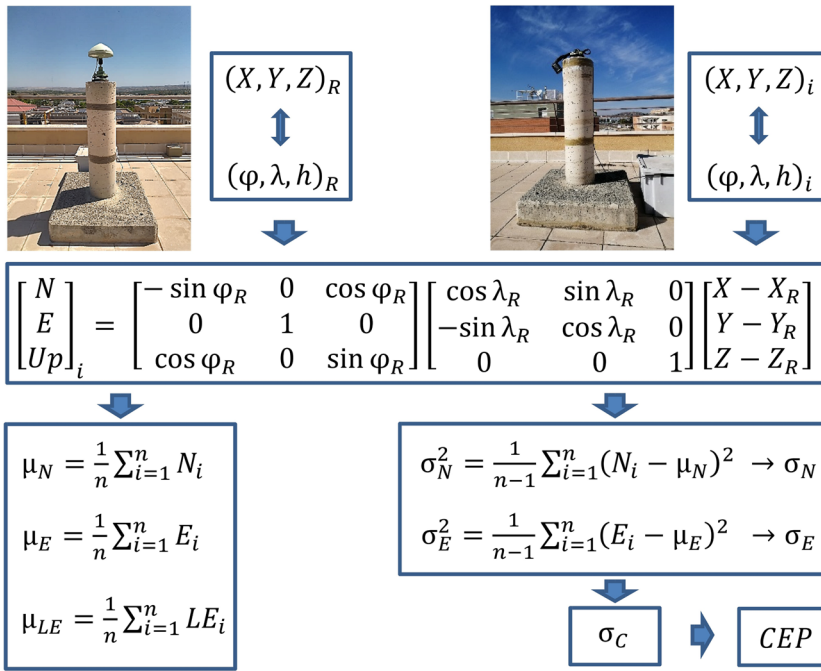


FIGURE 3 The flow diagram for transformation of the geocentric coordinates \$(X, Y, Z)\$ to geodetic coordinates (latitude \$[\varphi]\$, longitude \$[\lambda]\$, and ellipsoid height \$[h]\$), the estimation of the measurement error in the north and east components (\$N_i\$ and \$E_i\$) of the \$i\$th position registered by the global navigation satellite systems (GNSS) devices compared to the reference (R), the mean value of the measurement errors (\$\mu_N, \mu_E\$), the mean location error (\$\mu_{LE}\$), the standard deviations for the north and east component (\$\sigma_N\$ and \$\sigma_E\$), the circular standard deviation (\$\sigma_C\$), and the circular error probability (CEP).

TABLE 2 Repeatability of the evaluation parameters for the static test A of global navigation satellite system (GNSS) device performance carried out at the University of Jaén, Spain, during the sessions S1, S2, and S3 from 16–18 February 2021: number of successful fixes (\$n_f\$), fix success rate (FSR), mean location error (\$\mu_{LE}\$), circular standard deviation (\$\sigma_C\$), circular error probability (CEP), mean number of satellites used (SV), and mean horizontal dilution of precision (HDOP).

Test A Parameter	Low-cost GNSS receiver (LCR)			Multi-frequency GNSS collar (MFC)		
	S1	S2	S3	S1	S2	S3
\$n_f\$	48	48	48	48	48	48
FSR	100%	100%	100%	100%	100%	100%
\$\mu_{LE} \pm\$ SD (m)	\$0.464 \pm 0.247\$	\$0.526 \pm 0.286\$	\$0.751 \pm 0.331\$	\$1.36 \pm 0.79\$	\$1.40 \pm 0.89\$	\$1.36 \pm 0.81\$
\$\sigma_C\$ (m)	0.283	0.312	0.331	0.92	0.76	0.85
CEP (m)	0.334	0.367	0.389	1.09	0.90	1.00
SV \$\pm\$ SD	\$28 \pm 2.2\$	\$28 \pm 2.3\$	\$27 \pm 2.0\$	\$15 \pm 7.5\$	\$15 \pm 8.2\$	\$15 \pm 7.1\$
HDOP \$\pm\$ SD	\$0.5 \pm 0.1\$	\$0.5 \pm 0.1\$	\$0.5 \pm 0.1\$	\$0.9 \pm 0.2\$	\$0.9 \pm 0.2\$	\$0.8 \pm 0.2\$

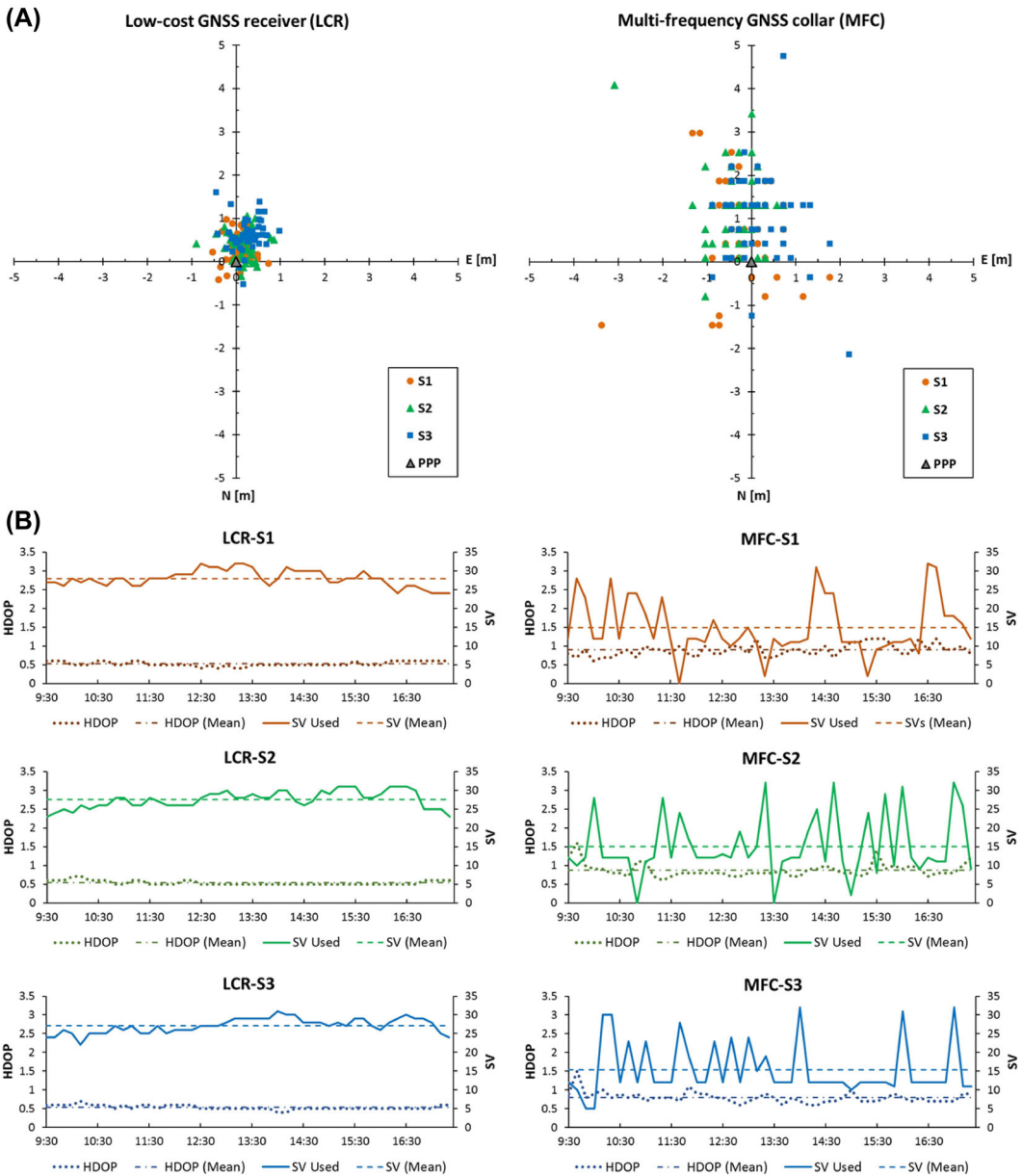


FIGURE 4 A) Scatter plots of location errors during the sessions S1, S2, and S3 for a low-cost global navigation satellite systems (GNSS) receiver (LCR; left) and for a multi-frequency GNSS collar (MFC; right). Vertical axis label (N) refers to the north direction and horizontal axis label (E) refers to the east direction. We used a precise point positioning (PPP) solution to establish the reference. B) Number of satellites (SV) and horizontal dilution of precision (HDOP) values by session (S1–S3) for the LCR (left) and the MFC (right). The horizontal axis shows the time in hours. We conducted static test A at the University of Jaén, Spain, from 16–18 February 2021.

from the LCR (Figure 4). The LCR had a circular error probability ranging from 0.334 m (S1) to 0.389 m (S3). This value varied from 0.90 m (S2) to 1.09 m (S1) for the MFC. For the MFC the mean location errors did not differ significantly between S1 and S2 ($t = -0.208, P = 0.835$), between S2 and S3 ($t = 0.198, P = 0.843$), or between S1 and S3 ($t = -0.007, P = 0.994$). For the LCR, the number of satellites doubled the values for the MFC (Table 2). The

TABLE 3 Results of the evaluation parameters for static test B of global navigation satellite system (GNSS) device performance carried out at the University of Jaén, Spain, 18 February (session S4) and 25 February (session S5) 2021: number of successful fixes (n_f), fix success rate (FSR), mean location error (μ_{LE}), circular standard deviation (σ_C), circular error probability (CEP), mean number of satellites used (SV), and mean horizontal dilution of precision (HDOP).

Test B Parameter	Multi-frequency GNSS collar (MFC) S4	Single-frequency GNSS collar (SFC) S5
n_f	144	144
FSR	100%	100%
$\mu_{LE} \pm SD$ (m)	1.15 ± 0.70	11.96 ± 13.05
σ_C (m)	0.83	12.39
CEP (m)	0.98	14.59
SV \pm SD	14 ± 6.6	8 ± 2.2
HDOP \pm SD	0.8 ± 0.1	1.3 ± 1.1

HDOP was always smaller than 2 for both GNSS devices (i.e., HDOP results indicated high quality fixes). A slight bias was present in the scatter plots for the positions registered by the MFC, more evident along the northern direction. This was due to the number of decimal places considered by the MFC. The LCR showed all of the digits registered in the NMEA sentence, whereas the MFC considered only 7 digits. The rounding to the nearest integer introduced a bias into the estimated coordinates close to the CEP associated with the ZED-F9P module used by the LCR, in this case at the 30-cm level.

In test B comparing stationary positions of the MFC and SFC, both collars demonstrated 100% fix success rates (Table 3). Clearly, the SFC presented a higher mean location error (11.96 m) than the MFC (1.15 m) and a smaller number of tracked satellites (Figure 5; Table 3), which had a direct impact on the HDOP values. The estimated circular standard deviation and the circular error probability were much greater for the SFC than the MFC (Table 3).

Kinematic tests

Sections of the routes R1 and R2 differed in canopy coverage, open sky, forest condition, and altitude (Figure 6). For R1 and R2, the positions for the MFC matched approximately with the reference track defined by the LCR; however, the positions deviated slightly from the reference path for the SFC (Figure 6A, B). For example, at one point, the distance between the SFC position and the reference track was 5.6 m (Figure 6B). This was approximately the mean distance to the reference track for this GNSS collar in R1. The maximum distance to the reference track for R2 considering the SFC solution was 16.8 m (Figure 6D). The MFC presented mean values for the relative location error <2 m, whereas the corresponding values for the SFC were around 5 m.

Three altimetric sections were clearly differentiated in R3 (Figure 7). For the MFC, the relative location error in a closed canopy environment with a complex topography was slightly greater than in an open environment. In both cases, the MFC presented a relative location error less than the SFC and the maximum distance to the reference track was 9.4 m for the SFC (Figure 7A) and 5.4 m for the MFC (Figure 7B).

Both GNSS collars achieved a 100% fix success rate in all routes and observation sessions (Table 4). The shortest distance from the MFC and the SFC to reference track R1 showed a mean value of 1.16 m and

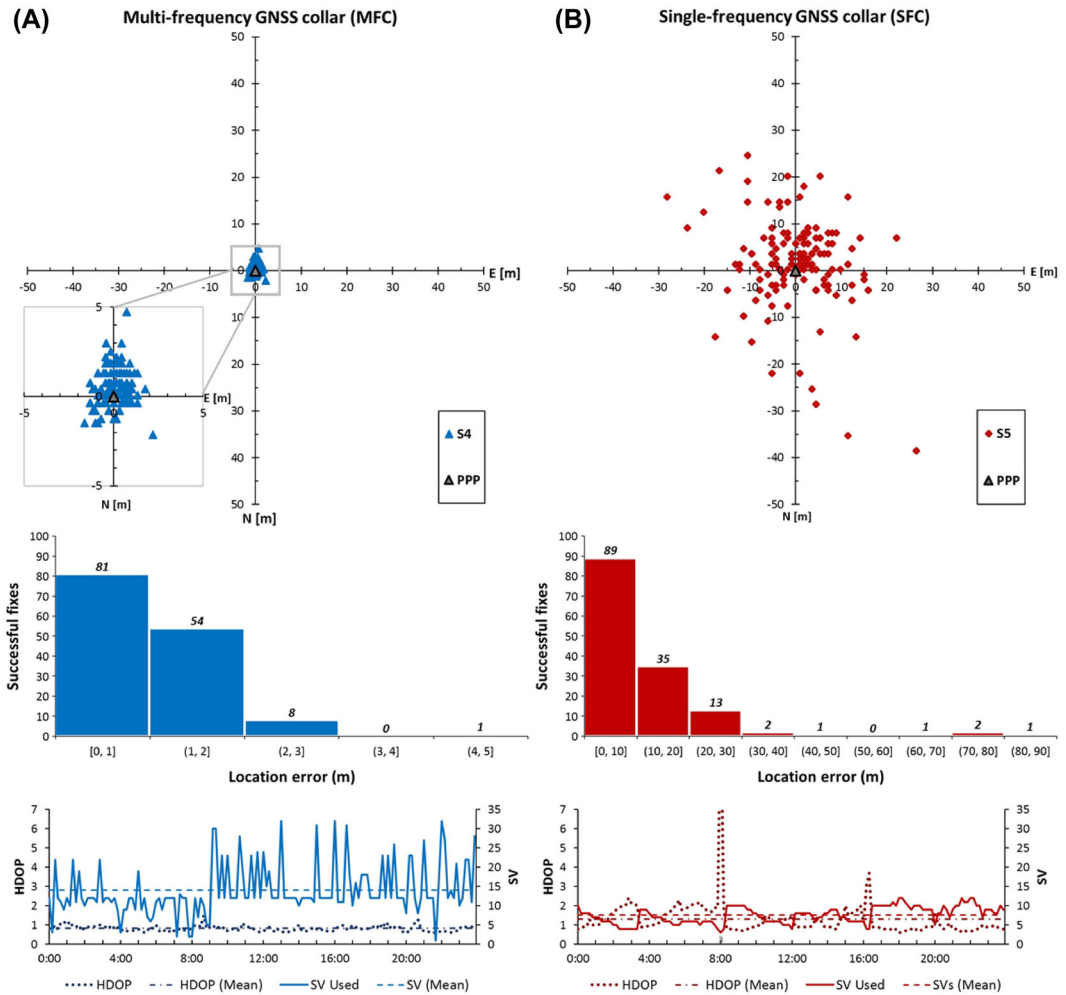


FIGURE 5 Scatter plots of location errors (vertical axis label N refers to the north direction and horizontal axis label E refers to the east direction) during the sessions S4 and S5, histogram of the location error, and number of satellites (SV) and horizontal dilution of precision (HDOP) values (horizontal axis shows the time in hours) for the multi-frequency global navigation satellite systems (GNSS) collar (MFC; A) and for the single-frequency GNSS collar (SFC; B). We used a precise point positioning (PPP) solution to establish the reference. In the SFC scatter plot, 4 records (largest values in the histogram) are outside the drawn error ranges and they are not visible. We conducted static test B at the University of Jaén, Spain, on 18–25 February 2021.

5.38 m, reaching maximum values of 2.21 m and 10.29 m, respectively. The number of satellites used was drastically reduced in these kinematic conditions for the SFC, affecting the HDOP values. For R2 (S7), the mean values of the shortest distance estimated to the reference track were 1.96 m for the MFC and 4.80 m for the SFC. The maximum values reached were 4.02 m and 16.80 m, respectively. The mean number of satellites used and HDOP values were similar for both collars in this session. The MFC kept stable the mean value of satellites used and HDOP values in R1 and R2. In our analysis of repeatability, the repeated session on route R2 (S8) indicated similar values to the previous session for the mean relative location error, the number of satellites, and the HDOP values. For R3 (S9), the SFC achieved very similar values to previous

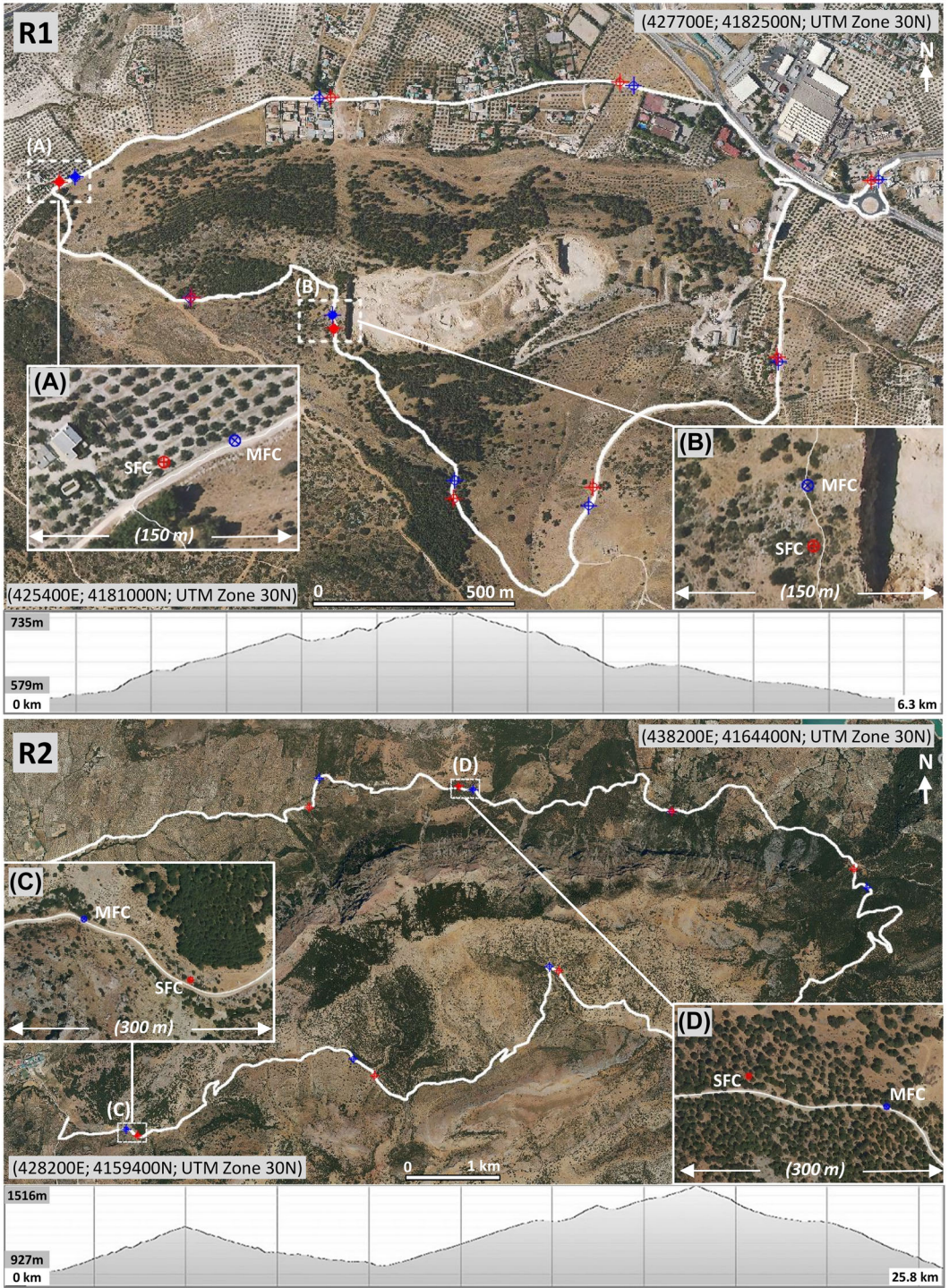


FIGURE 6 Planimetric and altimetric definition of route R1, on foot (session S6), and route R2, by car (session S7), with a low-cost global navigation satellite systems (GNSS) receiver (LCR; white line), a multi-frequency GNSS collar (MFC; blue dots), and a single-frequency GNSS collar (SFC; red dots). We conducted kinematic test C in Jaén, Spain, on 18–19 June 2021. Figure partially derived from orthophotographs of the Spanish National Orthophoto Program PNOA-2019 CC-BY, scene.es.

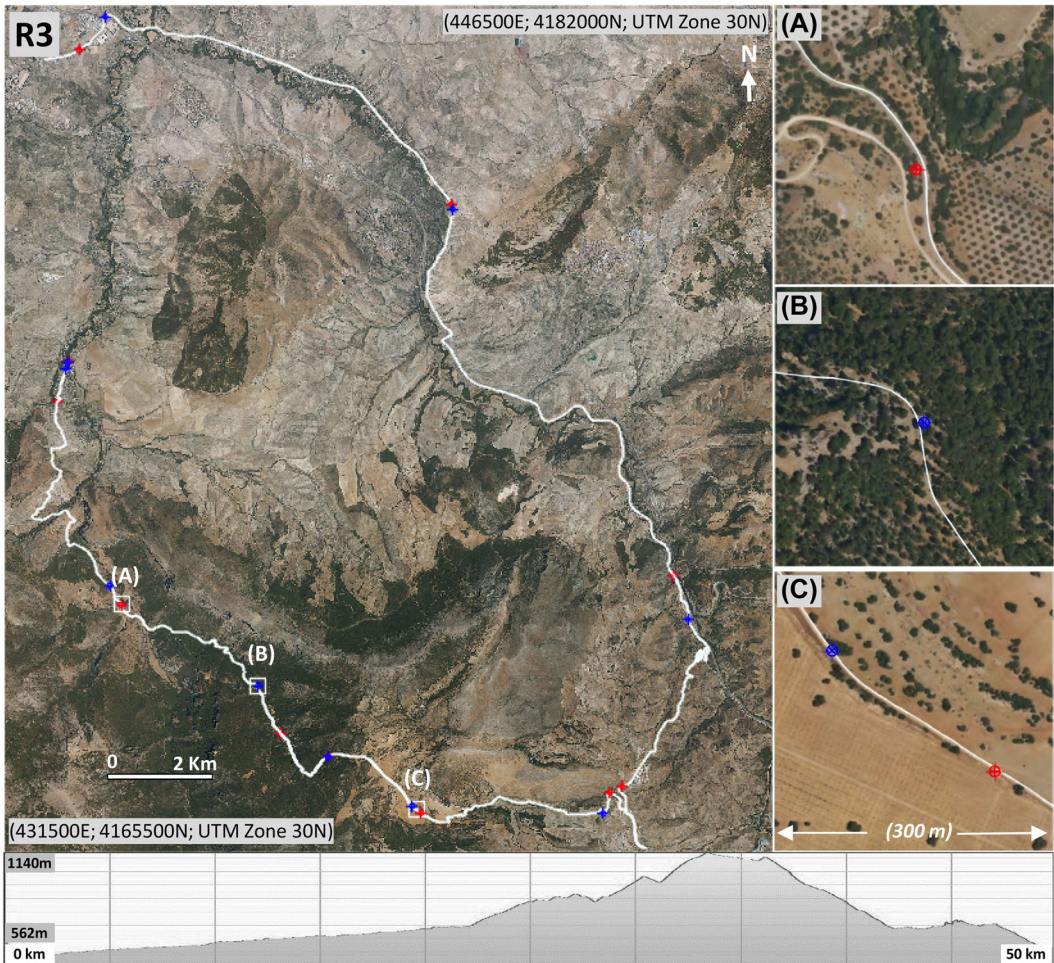


FIGURE 7 Planimetric and altimetric definition of route R3, by car (session S9), with a low-cost global navigation satellite systems (GNSS) receiver (LCR; white line), a multi-frequency GNSS collar (MFC; blue dots), and a single-frequency GNSS collar (SFC; red dots). We conducted kinematic test C in Jaén, Spain, on 20 June 2022. Figure partially derived from orthophotographs of the Spanish National Orthophoto Program PNOA-2019 CC-BY, scene.es.

sessions for the mean relative location, with a mean value equal to 4.75 m. This value was reduced to 2.09 m with the MFC.

DISCUSSION

We analyzed the reliability that newer GNSS technology can provide for use in wildlife applications. This work is a step forward with respect to previous tests of GPS collar performance carried out over the last decades (Cargnelutti et al. 2007, Yamazaki et al. 2009, Forin-Wiart et al. 2015, Schwartz et al. 2017). We confirmed the high performance of the new multi-frequency GNSS collar in static conditions. Nevertheless, the results suggested different performance in static mode for the LCR and the MFC, despite the fact that both are equipped with the same GNSS module and have been tested in very similar observation conditions. The MFC showed a close

TABLE 4 Results of the evaluation parameters for kinematic test C and routes R1 (18 June 2021, session S6), R2 (19 June 2021, session S7, and 20 June 2022, session S8), and R3 (21 June 2022, session S9) carried out in Jaén, Spain, with the multi-frequency global navigation satellite systems (GNSS) collar (MFC) and the single-frequency GNSS collar (SFC): number of successful fixes (n_f), fix success rate (FSR), relative location error (RLE), number of satellites used (SV), and horizontal dilution of precision (HDOP).

Test C Parameter	Route R1		Route R2				Route R3	
	S6		S7	S8	S8	S9	S9	
	MFC	SFC	MFC	SFC	MFC	SFC	MFC	SFC
n_f	9	9	8	8	10	10	10	10
FSR (%)	100	100	100	100	100	100	100	100
RLE (m)								
Min.	0.07	3.35	0.34	0.01	0.19	0.02	0.20	0.15
Max.	2.21	10.29	4.02	16.80	3.36	12.91	5.43	9.38
\bar{x}	1.16	5.38	1.96	4.80	1.16	4.72	2.09	4.75
SD	0.74	2.47	1.31	5.33	0.96	4.53	1.67	3.49
SV used								
Min.	9	4	7	7	8	5	5	5
Max.	12	4	12	9	11	7	12	7
\bar{x}	12	4	10	8	9	6	10	6
SD	1	0	2	1	1	1	3	1
HDOP								
Min.	0.8	1.8	0.7	1.0	0.8	1.0	0.8	1.0
Max.	1.2	2.6	2.1	1.7	1.7	1.6	2.6	1.9
\bar{x}	0.9	2.0	1.3	1.3	1.3	1.4	1.3	1.4
SD	0.2	0.3	0.5	0.3	0.2	0.2	0.6	0.3

agreement with the CEP reported by the manufacturer of the ZED-F9P module. The number of satellites used by the MFC was almost half that used by the LCR. Additional tests will be carried out in the future to better understand and explain this aspect. The LCR showed better performance than the MFC, probably because of the high-frequency sampling rate and the advanced jamming and spoofing detection technologies applied by the LCR. Both GNSS devices presented a homogeneous performance throughout the observation sessions. Based on the static tests, the MFC is characterized by a stable and better performance than the SFC in terms of precision, accuracy, and GNSS satellite tracking capability. In view of the results, we confirm that the circular standard deviation and the circular error probability were better by approximately one order of magnitude for the MFC compared to the SFC. The results of both GNSS collars were consistent with those stated by the manufacturer of the GNSS modules.

We conducted the kinematic test in a forest environment to test the GNSS collars in motion. Again, the MFC showed a better performance than the SFC, with a mean value of relative location error approximately 3 times lower than the SFC. The number of satellites is drastically reduced in kinematic conditions for the SFC, affecting the HDOP values. Even at locations under an obstructed sky environment, due to the presence of dense vegetation, the MFC showed a better performance in terms of relative accuracy than the SFC. Although the MFC has shown more accurate results than the SFC, in next phases of testing the kinematic test will be repeated at a finer fix rate and for a longer period time to describe the MFC error patterns in both open and closed canopy environments.

There are still several challenges in this research, including the quality analysis of the GNSS raw measurements, the design of optimal and smaller GNSS devices, the implementation of the differential correction algorithms to improve the accuracy of the collar positions, the analysis of GNSS collars settings, and the environment effects on the collar data solutions. Nevertheless, the use of these reliable and accurate GNSS devices will allow us to expand the knowledge of animal behavior and the interactions between species in a specific study area. The prototype multi-constellation multi-frequency GNSS collar has been specially designed to monitor Iberian red deer (*Cervus elaphus hispanicus*) and fallow deer (*Dama dama*) in sympatric wild populations in southern Spain (Azorit et al. 2012) to explain the different feeding strategies of both species and to better understand whether the large diet overlap detected involves interspecific competition for resources. Furthermore, this GNSS collar can be adapted to other wild mammals to obtain accurate data for behavioral analyses with approaches that already consider heterogeneity and the 3 dimensions of the landscape (Valderrama-Zafra et al. 2022).

The development in remote sensing technologies will increase the availability of spatially continuous information, facilitating a more widespread use of structural vegetation variables in habitat modeling and hence improving conservation planning (Gastón et al. 2019). Another important research issue is the combination of GNSS technology and the fine-scale spatial information provided by the advances in remote monitoring through cameras on unmanned aerial vehicles, and the use of GNSS devices providing precise real-time locations. The accurate determination of ground locations combined with remotely acquired images allows researchers to analyze nearly in real time the interactions between animals and the landscape.

RESEARCH IMPLICATIONS

In wildlife management, many studies now opt to record positions and parameters at a high sampling frequency at the cost of reduced battery life. The resolution with which GNSS devices and collars can define fine-scale movement mainly depends on the precision and the accuracy achieved by them. Although the SFC can be applied in studies focused on the examination of home ranges or habitat use, the results showed that the MFC allowed collecting accurate locations (CEP ~ 1 m), providing fine-scale information about animal behavior. The MFC performance makes it suitable for applications that require high accuracy and a high temporal resolution such as the determination of social interactions, assessment of habitat preferences, identification of revisited locations, explanation of feeding strategies in sympatric wild populations, or better knowledge of the competition for resources. The availability of reliable, accurate, and remote-download GNSS collars provides new opportunities for studying movement and space-use patterns, incorporating this accurate spatial information into wildlife research projects, conservation actions, and management programs.

ACKNOWLEDGMENTS

We thank the editor, the associate editor, and the anonymous reviewers for their valuable comments and the helpful feedback that improved this manuscript. The support provided by Microsensory S.L. Company in the design and manufacturing the GNSS collars is gratefully acknowledged. This study was funded by the University of Jaén (Programa Operativo FEDER Andalucía 2014-2020 - Project 1263446 - call made by UJA 2018, POAIUJA 2021-2022, CECTEMA and funding for open access charge: Universidad de Jaén/CBUA), Junta de Andalucía (Plan Andaluz de Investigación, Desarrollo e Innovación PAIDI2020 - Project P20-00897, Project P07-RNM-03087, Research Groups RNM175 and RNM282), and MINECO of Spain (Project CGL2016-78577-P).

CONFLICTS OF INTEREST STATEMENT

The authors declare no conflicts of interest.

ETHICS STATEMENT

This manuscript does not analyse data derived from studies with animals.

DATA AVAILABILITY STATEMENT

Data available on request due to privacy/ethical restrictions: The data that support the findings of this study are available on request from the corresponding author. The data are not publicly available due to privacy or ethical restrictions.

ORCID

María S. Garrido-Carretero  <http://orcid.org/0000-0001-8914-9431>

REFERENCES

- Alonso, M. T., J. Sanz, J. M. Juan, A. Rovira, and G. G. Casado. 2020. Galileo broadcast ephemeris and clock errors analysis: 1 January 2017 to 31 July 2020. *Sensors* 20:6832.
- Awange, J. 2018. *GNSS environmental sensing: revolutionizing environmental monitoring*. Springer, Cham, Switzerland.
- Azorit, C., S. Tellado, A. Oya, and J. Moro. 2012. Seasonal and specific diet variations in sympatric red and fallow deer of southern Spain. *Animal Production Science* 52:720–727.
- Barzaghi, R., N. E. Cazzaniga, C. L. De Gaetani, L. Pinto, and V. Tornatore. 2018. Estimating and comparing dam deformation using classical and GNSS techniques. *Sensors* 18:756–766.
- Bengsen, A. J., J. O. Hampton, S. Comte, S. Freney, and D. M. Forsyth. 2021. Evaluation of helicopter net-gunning to capture wild fallow deer (*Dama dama*). *Wildlife Research* 48:722–729.
- Bowman, J. L., C. O. Kochanny, S. Demarais, and B. D. Leopold. 2000. Evaluation of a GPS collar for white-tailed deer. *Wildlife Society Bulletin* 28:141–145.
- Cain, J. W., P. R. Krausman, B. D. Jansen, and J. R. Morgart. 2005. Influence of topography and GPS fix interval on GPS collar performance. *Wildlife Society Bulletin* 33:926–934.
- Caporali, A., and J. Zurutuza. 2021. Broadcast ephemeris with centimetric accuracy: test results for GPS, Galileo, Beidou and Glonass. *Remote Sensing* 13:4185.
- Cargnelutti, B., A. Coulon, A. J. M. Hewison, M. Goulard, J. Angibault, and N. Morellet. 2007. Testing global positioning system performance for wildlife monitoring using mobile collars and known reference points. *Journal of Wildlife Management* 71:1380–1387.
- Dardanelli, G., A. Maltese, C. Pipitone, A. Pisciotta, and M. Lo Brutto. 2021. NRTK, PPP or static, that is the question. Testing different positioning solutions for GNSS survey. *Remote Sensing* 13:1406–1435.
- Davis, G. H., M. C. Crofoot, and D. R. Farine. 2018. Estimating the robustness and uncertainty of animal social networks using different observational methods. *Animal Behaviour* 141:29–44.
- Dion, J. R., J. M. Haus, J. E. Rogerson, and J. L. Bowman. 2019. An initial performance review of vaginal implant transmitters paired with GPS collars. *Animal Biotelemetry* 7:22.
- Fischer, M., K. Parkins, K. Maizels, D. R. Sutherland, B. M. Allan, G. Coulson, and J. Di Stefano. 2018. Biotelemetry marches on: a cost-effective GPS device for monitoring terrestrial wildlife. *PLoS ONE* 13:e0199617.
- Forin-Wiart, M.-A., P. Hubert, P. Sirguey, and M. L. Poulle. 2015. Performance and accuracy of lightweight and low-cost GPS data loggers according to antenna positions, fix intervals, habitats and animal movements. *PLoS ONE* 10:e0129271.
- Frair, J. L., J. Fieberg, M. Hebblewhite, F. Cagnacci, N. De Cesare, and L. Pedrotti. 2010. Resolving issues of imprecise and habitat-biased locations in ecological analyses using GPS telemetry data. *Philosophical Transactions of the Royal Society B* 365:2187–2200.
- Gao, X., W. Dai, Z. Song, and C. Cai. 2017. Reference satellite selection method for GNSS high-precision relative positioning. *Geodesy and Geodynamics* 8:125–129.
- Gao, W., S. Pan, C. Gao, Q. Wang, and R. Shang. 2019. Tightly combined GPS and GLONASS for RTK positioning with consideration of differential inter-system phase bias. *Measurement Science and Technology* 30:054001.
- Garrido, M. S., M. C. de Lacy, M. J. Borque, A. M. Ruiz, R. Moreno, and A. J. Gil. 2019. Low-cost GNSS receiver in RTK positioning under the standard ISO-17123-8: a feasible option in geomatics. *Measurement* 137:168–178.
- Garrido, M. S., M. C. de Lacy, and A. M. Rojas. 2018. Impact of tropospheric modelling on GNSS vertical precision: an empirical analysis based on a local active network. *International Journal of Digital Earth* 11:880–896.
- Gastón, A., S. Blázquez-Cabrera, C. Ciudad, M. C. Mateo-Sánchez, M. A. Simón, and S. Saura. 2019. The role of forest canopy cover in habitat selection: insights from the Iberian lynx. *European Journal of Wildlife Research* 65:30.
- Gelb, A. 1974. *Applied optimal estimation*. The M. I. T. Press, Cambridge, Massachusetts, USA and London, England.

- Geng, J., and J. Guo. 2020. Beyond three frequencies: an extendable model for single-epoch decimeter-level point positioning by exploiting Galileo and BeiDou-3 signals. *Journal of Geodesy* 94:14.
- Ghilani, C. D., and P. R. Wolf. 2010. *Adjustment computations: spatial data analysis*. John Wiley & Sons, Hoboken, New Jersey, USA.
- Grala, N., and M. Brach. 2009. Analysis of GNSS receiver accuracy in the forest environment. *Annals of Geomatics* 7:41–47.
- Gray, S. M., J. M. Humphreys, R. A. Montgomery, D. R. Etter, K. C. VerCauteren, B. D. Kramer, and G. J. Roloff. 2022. Behavioral states in space and time: understanding landscape use by an invasive mammal. *Journal of Wildlife Management* 86:e22211.
- Greenwalt, C. R., and M. C. Shultz. 1962. *Principles of error theory and cartographic applications*. ACIC Technical Report No. 96. Aeronautical Chart and Information Center, St. Louis, Missouri, USA.
- Hampton, J. O., M. Amos, A. Pople, M. Brennan, and D. M. Forsyth. 2020. Minimising mortalities in capturing wildlife: refinement of helicopter darting of chital deer (*Axis axis*) in Australia. *Wildlife Research* 48:304–313.
- Hamza, V., B. Stopar, and O. Sterle. 2021. Testing the performance of multi-frequency low-cost GNSS receivers and antennas. *Sensors* 21:2029.
- Hofmann-Wellenhof, B., H. Lichtenegger, and E. Wasle. 2008. *GNSS—Global Navigation Satellite Systems: GPS, GLONASS, Galileo, and more*. Springer-Verlag, Wien, Austria.
- Hooven, N. D., K. E. Williams, J. T. Hast, J. R. McDermott, R. D. Crank, G. Jenkins, M. T. Springer, and J. J. Cox. 2022. Using low-fix rate GPS telemetry to expand estimates of ungulate reproductive success. *Animal Biotelemetry* 10:5.
- International Organization for Standardization. 2012. *International vocabulary of metrology – basic and general concepts and associated terms (VIM)*. Third edition. International Organization for Standardization, Geneva, Switzerland.
- Irvine, C. C., S. G. Cherry, and B. R. Patterson. 2022. Discriminating grey wolf kill sites using GPS clusters. *Journal of Wildlife Management* 86:e22163.
- Janos, D., and P. Kuras. 2021. Evaluation of low-cost GNSS receiver under demanding conditions in RTK network mode. *Sensors* 21:5552.
- Laguna, E., A. J. Carpio, J. Vicente, J. A. Barasona, R. Triguero-Ocaña, S. Jiménez-Ruiz, A. Gómez-Manzaneque, and P. Acevedo. 2021. The spatial ecology of red deer under different land use and management scenarios: Protected areas, mixed farms and fenced hunting estates. *Science of the Total Environment* 786:1–9.
- Leica Geosystems. 2011. *Leica GNSS network and reference stations - technical data*. Leica Geosystems AG, Heerbrugg, Switzerland.
- Li, X., J. Huang, X. Li, H. Lyu, B. Wang, Y. Xiong, and W. Xie. 2021. Multi-constellation GNSS PPP instantaneous ambiguity resolution with precise atmospheric corrections augmentation. *GPS Solution* 25:1–13.
- Li, X., B. Wang, X. Li, J. Huang, H. Lyu, and X. Han. 2022. Principle and performance of multi-frequency and multi-GNSS PPP-RTK. *Satellite Navigation* 3:7.
- Liu, T., B. Zhang, Y. Yuan, and X. Zhang. 2020. On the application of the raw-observation-based PPP to global ionosphere VTEC modeling: an advantage demonstration in the multi-frequency and multi-GNSS context. *Journal of Geodesy* 94:1–20.
- Marchand, P., M. Garel, N. Morellet, L. Benoit, Y. Chaval, C. Itty, E. Petit, B. Cargnelutti, A. J. M. Hewison, and A. Loison. 2021. A standardized biologging approach to infer parturition: an application in large herbivores across the hider-follower continuum. *Methods in Ecology and Evolution* 12:1017–1030.
- Meyer, T. H. 2010. *Introduction to geometric and physical geodesy: foundations of geomatics*. ESRI Press, Redlands, California, USA.
- Moriarty, K. M., and C. W. Epps. 2015. Retained satellite information influences performance of GPS devices in a forested ecosystem. *Wildlife Society Bulletin* 2:349–357.
- Pan, L., X. Zhang, X. Li, C. Lu, J. Liu, and Q. Wang. 2019. Satellite availability and point positioning accuracy evaluation on a global scale for integration of GPS, GLONASS, BeiDou and Galileo. *Advances in Space Research* 63:2696–2710.
- Paziewski, J., M. Fortunato, A. Mazzoni, and R. Odolinski. 2021. An analysis of multi-GNSS observations tracked by recent Android smartphones and smartphone-only relative positioning results. *Measurement* 175:1–16.
- Peterson, C. J., N. J. DeCesare, T. A. Hayes, C. Bishop, and M. S. Mitchell. 2022. Consequences of migratory strategy on habitat selection by mule deer. *Journal of Wildlife Management* 86:e22135.
- Pipitone, C., A. Maltese, G. Dardanelli, M. L. Brutto, and G. L. Loggia. 2018. Monitoring water surface and level of a reservoir using different remote sensing approaches and comparison with dam displacements evaluated via GNSS. *Remote Sensing* 10:71–95.
- Psychas, D., P. J. G. Teunissen, and S. Verhagen. 2021. A multi-frequency Galileo PPP-RTK convergence analysis with an emphasis on the role of frequency spacing. *Remote Sensing* 13:3077.
- Rodgers, A. R. 2001. Tracking animals with GPS: the first 10 years. Pages 1–10 in *Proceedings of the Conference on Tracking Animals with GPS*. The Macaulay Land Use Research Institute, 12–13 March 2001, Aberdeen, Scotland.
- Rodgers, A. R., R. S. Rempel, and K. F. Abraham. 1996. A GPS-based telemetry system. *Wildlife Society Bulletin* 24: 559–566.

- Schwartz, C. C., S. Podrutzny, S. L. Cain, and S. Cherry. 2017. Performance of spread spectrum global positioning system collars on grizzly and black bears. *Journal of Wildlife Management* 73:1174–1183.
- Seeber, G. 2003. *Satellite geodesy: foundations, methods and applications*. Walter de Gruyter GmbH & Co., Berlin, Germany.
- Takasu, T. 2010. Real-time PPP with RTKLIB and IGS real-time satellite orbit and clock. IGS Workshop 2010, 28 June–2 July, 2010, Newcastle upon Tyne, England.
- Taylor, B. N., and C. E. Kuyatt. 1994. *Guidelines for evaluating and expressing the uncertainty of NIST measurement results*. NIST Technical Note 1297. National Institute of Standards and Technology, Gaithersburg, Maryland, USA.
- Teunissen, P. J. G. 2000. *Testing theory: an introduction*. VSSD, Delft, South Holland, Netherlands.
- Teunissen, P. J. G., and O. Montenbruck. 2017. *Springer handbook of global navigation satellite systems*. Springer International Publishing, Cham, Switzerland.
- Tunini, L., D. Zuliani, and A. Magrin. 2022. Applicability of cost-effective GNSS sensors for crustal deformation studies. *Sensors* 22:350.
- U-blox AG. 2013. ITM530M Fastrax GPS/GNSS module. Document number FTX-HW-12001-3. <<https://www.u-blox.com>>. Accessed 21 Dec 2022.
- U-blox AG. 2020. ZED-F9P. U-blox F9 high precision GNSS module. Document number UBX-17051259-R08. <<https://www.u-blox.com>>. Accessed 21 Dec 2022.
- U-blox AG. 2021a. Product summary ZED-F9P module. Document number UBX-17005151-R10. <<https://www.u-blox.com>>. Accessed 21 Dec 2022.
- U-blox AG. 2021b. U-center GNSS evaluation software for windows. Document number UBX-13005250-R23. <<https://www.u-blox.com>>. Accessed 21 Dec 2022.
- Valderrama-Zafra, J. M., P. Fernández-Rodríguez, A. Oya, R. Carrasco, M. A. Rubio-Paramio, M. S. Garrido-Carretero, and C. Azorit. 2022. Assessing 3D vs. 2D habitat metrics in a Mediterranean ecosystem for a wiser wildlife management. *Ecological Informatics* 69:101623.
- Weiss, P. 2021. Welcome to the Global Navigation Multi-Constellation. *Engineering* 7:421–423.
- Wielgocka, N., T. Hadas, A. Kaczmarek, and G. Marut. 2021. Feasibility of using low-cost dual-frequency GNSS receivers for land surveying. *Sensors* 21:1956.
- Wielgus, E., A. Caron, E. Bennitt, M. De Garine-Wichatitsky, B. Cain, H. Fritz, E. Eve Miguel, D. Cornélis, and S. Chamailé-Jammes. 2021. Inter-group social behavior, contact patterns and risk for pathogen transmission in cape buffalo populations. *Journal of Wildlife Management* 85:1574–1590.
- Wittemyer, G., M. Northrup, and G. Bastille-Rousseau. 2019. Behavioral valuation of landscapes using movement data. *Philosophical Transactions of the Royal Society B: Biological Sciences* 374:1520180046.
- Xiao, R., H. Shi, X. He, Z. Li, D. Jia, and Z. Yang. 2019. Deformation monitoring of reservoir dams using GNSS: an application to South-to-North Water Diversion Project, China. *IEEE Access* 7:54981–54992.
- Xin, S., J. Geng, J. Guo, and X. Meng. 2020. On the choice of the third-frequency Galileo signals in accelerating PPP ambiguity resolution in case of receiver antenna phase center errors. *Remote Sensing* 12:1315.
- Xu, G. 2007. *GPS: theory, algorithms, and applications*. Springer-Verlag, Berlin, Germany.
- Yamazaki, K., S. Kasai, S. Koike, Y. Goto, C. Kozakai, and K. Furubayashi. 2009. Evaluation of GPS collar performance by stationary tests and fitting on free-ranging Japanese black bears. *Mammal Study* 33:131–142.
- Zumberge, J. F., M. B. Heflin, D. C. Jefferson, M. M. Watkins, and F. H. Webb. 1997. Precise point positioning for the efficient and robust analysis of GPS data from large networks. *Journal of Geophysical Research* 102:5005–5017.

Associate Editor: Francesco Ferretti.

How to cite this article: Garrido-Carretero, M. S., C. Azorit, M. C. de Lacy-Pérez de los Cobos, J. M. Valderrama-Zafra, R. Carrasco, and A. J. Gil-Cruz. 2023. Improving the precision and accuracy of wildlife monitoring with multi-constellation, multi-frequency GNSS collars. *Journal of Wildlife Management* e22378. <https://doi.org/10.1002/jwmg.22378>